Development 128, 2793-2802 (2001)
Printed in Great Britain © The Company of Biologists Limited 2001
DEV5916

The *furry* gene of *Drosophila* is important for maintaining the integrity of cellular extensions during morphogenesis

Jingli Cong, Wei Geng*, Biao He, Jingchun Liu, Jeannette Charlton and Paul N. Adler‡

Biology Department and Cancer Center, University of Virginia, Charlottesville, VA 22903, USA
*Present address: Immunology Department, Genencor International, Inc., 925 Page Mill Road, Palo Alto, CA 94304, USA
‡Author for correspondence (e-mail: pna@virginia.edu)

Accepted 5 May 2001

SUMMARY

The *Drosophila* imaginal cells that produce epidermal hairs, the shafts of sensory bristles and the lateral extensions of the arista are attractive model systems for studying the morphogenesis of polarized cell extensions. We now report the identification and characterization of *furry*, an essential *Drosophila* gene that is involved in maintaining the integrity of these cellular extensions during morphogenesis. Mutations in *furry* result in the formation of branched arista laterals, branched bristles and a strong multiple hair cell phenotype that consists of clusters of epidermal hairs and branched hairs. By following the morphogenesis of arista laterals in pupae, we have determined that the branched laterals are due to the splitting of individual laterals during elongation. In genetic mosaics *furry* was found to act cell autonomously in the wing. The phenotypes of double mutant cells argue that *furry* functions independently of the *frizzled* planar polarity pathway and that it probably functions in the same pathway as the *tricornered* gene. We used a P-element insertion allele as a tag to clone the *furry* gene and found it to be a large and complicated gene that encodes a pair of large conserved proteins of unknown biochemical function.

Key words: *furry*, Morphogenesis, Actin cytoskeleton, *Drosophila*

INTRODUCTION

The adult cuticular surface of *Drosophila* is decorated with large numbers of polarized structures such as sensory bristles and epidermal hairs. The development of these structures has been actively studied as a model for the morphogenesis of highly polarized cellular components (Tilney et al., 2000b; Turner and Adler, 1998). Not surprisingly, these structures contain prominent cytoskeletal elements. Developing hairs and bristles contain actin filaments and microtubules and the function of both is required for normal morphogenesis (Eaton et al., 1996; Turner and Adler, 1998; Tilney et al., 1995).

The large size of the sensory bristle shaft cells has made them an attractive system for microscopic observations (Tilney et al., 1995). Developing bristles contain a series of large bundles of actin filaments located peripherally and juxtaposed to the plasma membrane (Tilney et al., 1996). The bundles are assembled in modules at the distal tip of the shaft. There appear to be two crosslinking systems that are used to assemble the large bundles (Tilney et al., 1995; Tilney et al., 1998). A primary bundling requires the function of the *forked* (*f*) gene (Petersen et al., 1994) and a second crosslinking requires the function of the *singed* (*sn*) gene (which encodes a fascin; Cant et al., 1994; Bryan et al., 1993). Mutations in either of these genes results in short, twisted and bent bristles. In *sn f* double mutants, the large bundles of actin filaments are lost, although a small number of actin filaments remain juxtaposed to the plasma membrane (Tilney et al., 1998). Interestingly the phenotype of the double mutant is not substantially stronger than either single mutant. Hence, the large bundles of actin filaments are not essential for bristle outgrowth, but they do appear to be important for the development of a normal length and shape. Microtubules are found centrally located in developing bristles and, based on their location, seem likely to be involved in bristle morphogenesis (Tilney et al., 1995); but genetic data that prove this are not available.

Epidermal hairs are outgrowths of individual cells and are much smaller than the shafts of sensory bristles. Epidermal hairs have primarily been studied on the pupal wing, where each cell forms a single hair (Wong and Adler, 1993). Growing hairs stain strongly for F-actin and tubulin (Eaton et al., 1996; Wong and Adler, 1993; Turner and Adler, 1998). There is no evidence for large bundles of actin filaments, but mutations in genes that encode bundling proteins such as *sn* and *f* produce mutant phenotypes (bent hairs), suggesting that actin bundling has a role in hair morphogenesis. Confocal and electron microscopy (EM) studies indicate that the microtubules are centrally located and that F actin is peripherally located in growing hairs (Turner and Adler, 1998), however, it is not clear if the arrangement is as defined as in the bristles. The lateral side branches of the arista are a third type of polarized cuticular structure with many similarities to hairs and bristles. Elongating laterals stain strongly for actin and EM studies shows the presence of bundles of actin filaments. These laterals

also contain centrally localized microtubules; thus, developing laterals are quite similar to bristles shafts in morphology (He and Adler, 2001). The development of the arista laterals has not been well studied but many mutations that alter hair and bristle morphology also alter lateral morphology (B. H. and P. N. A., unpublished).

Genetic studies on bristle and hair morphogenesis have been complemented by inhibitor studies using either in vitro organ culture of pupal wings and thoraces or the injection of inhibitors into appropriately aged pupae (Turner and Adler, 1998; Tilney et al., 2000a; Geng et al., 2000). The inhibition of actin polymerization by cytochalasin D (CD) has several effects on wing hair development. The initiation of hair morphogenesis is delayed, hair elongation is slowed, hairs end up shorter than normal, and hair clusters and split hairs are seen (Turner and Adler, 1998). Similarly, bristle outgrowth is delayed, bristle elongation is slowed, and adult bristles are short, bent and frequently split after the application of CD or lantrunculin A (LAT A; Geng et al., 2000; Tilney et al., 2000a). In at least some cases, the splitting appears to be due to ectopic initiation of bristle outgrowths either from 'budding' along the shaft of an existing bristle or from the apical surface of the cell. CD treatment also delays and slows arista lateral outgrowth and results in short and frequently split laterals (He and Adler, 2001).

The application of microtubule antagonists, such as vinblastine (VB) or colchicine (CH) produces an overlapping but distinct set of phenotypes in all three of these cell types. The rate of wing hair elongation is slowed, but in contrast to the results with CD, hair initiation is not delayed (Turner and Adler, 1998). VB and CH treatment leads to the formation of multiple hair cells. The hairs however are not clustered as tightly as those seen after treatment with CD. The injection of VB or CH into pupae results in short and fat bristles (Geng et al., 2000; see Tilney et al., 2000a for a different result). In addition to this dramatic stunting VB also causes bent and occasionally split bristles.

Mutations in the *tricornered* (*trc*) gene, which encodes the *Drosophila* NDR (nuclear DBF2 related) kinase, result in dramatic multiple wing hair, branched bristle and arista lateral phenotypes (Geng et al., 2000). These phenotypes are distinct from those produced by the antagonism of the actin or microtubule cytoskeletons in that *trc* hairs, bristles and laterals are not shortened and thickened as are those treated with inhibitors. The phenotype of *trc* bristles also differs from those seen in mutants for actin-bundling proteins such as *singed* or *forked*, because in these mutants bristle morphology is abnormal all along the length of the bristle. By contrast, the morphology of *trc* bristles is usually normal at 'non-branched' locations along the bristle shaft. Based on these differences, we previously proposed that *trc* did not encode a cytoskeletal component required for bristle morphogenesis, but rather that it encoded a protein that had a subtle interaction with the cytoskeleton (Geng et al., 2000). One possibility is that it is involved in coordinating multiple cellular components during morphogenesis.

We now report the recovery and characterizations of mutations in a new cell autonomously acting gene, named *furry* (*fry*) that yields a *trc*-like phenotype in bristles, hairs and laterals. The phenotypic similarities seen in the adult structures extend to the developing pupal epidermis suggesting that *trc* and *fry* might function in the same process. Consistent with this possibility, we found that *fry trc* double mutant cells did not show a stronger phenotype than either single mutant. Compelling evidence that *fry* results in the splitting of laterals was obtained by in vivo observation of developing laterals. We have cloned and characterized the *fry* gene using a P insertion allele, RT-PCR, mutant gene sequencing and cDNA clone analysis. We found that *fry* is a large and complicated gene that encodes two proteins. One protein contains 3479 amino acids and the second is a truncated version of this. Homologs of Fry are found in humans, *Caenorhabditis elegans*, *Arabidopsis* and yeast, but nothing is known about the biochemical function of the homologs.

MATERIALS AND METHODS

Fly culture and strains

Flies were grown on standard media. Many mutant and Deficiency-containing stocks, and P-insertion mutants were obtained from the stock center at Indiana University. The GMR-*sina* stock was kindly supplied by Gerry Rubin's laboratory (Neufeld et al., 1998).

Cytological procedures

The process of wing hair morphogenesis was studied as described previously (Turner and Adler, 1998). The morphogenesis of other body regions and cell types was studied in a similar manner. Adobe Photoshop was used to compose bitmap figures, and Corel Draw was used to compose line drawings. Confocal images were obtained using a BioRad confocal microscope at the Keck Center for Cellular Imaging at the University of Virginia. Other images were obtained using a Spot digital camera (National Diagnostics) on a Zeiss Axioskop 2 microscope.

Molecular characterization of *fry*

The *fry* cDNA and mRNA were assembled by a combination of cDNA clone isolation and PCR analysis of cDNA preparations. cDNA clones were isolated from the region from exon 3 to 14. The largest of these was more than 4 kb. This clone was sequenced and compared with genomic sequence from the BDGP/Celera project (Adams et al., 2000) and from sequencing in the region that we did independently. A cDNA from the 3′ end of *fry* (SD10447) was identified as a genome project EST clone. This was obtained from Research Genetics, sequenced and the sequence compared with genomic sequence. To identify the remaining exons and to ensure that all of the exons were linked up as predicted, we scanned the sequence to identify potential coding region and, using primers from these regions, we amplified cDNA from the imaginal disc cDNA library constructed by Brown and Kafatos (Brown and Kafatos, 1988). The PCR products were sequenced and the results used to pick new PCR primers to continue the walk. Eleven overlapping regions were amplified and sequenced in this way. In these experiments, we only obtained evidence for the mRNA that encodes the long form of Fry (*fry-l* mRNA). Evidence for the alternative *fry-s*, mRNA came from a cDNA clone. When we used primers specific for *fry-s*, we were able to detect it by RT-PCR. Northern blot analysis was carried out as described previously (Geng et al., 2000). We also used the *Drosophila* Rapid Scan cDNA panel (Origene Technologies) to examine the expression of *fry*.

Generation of genetic mosaics

Mosaic clones were generated using the FLP/FRT system (Golic and Lindquist, 1989; Xu and Rubin, 1993).

Scoring of mutant wings

Wings were mounted in Euparal (Asco Labs) and examined by bright

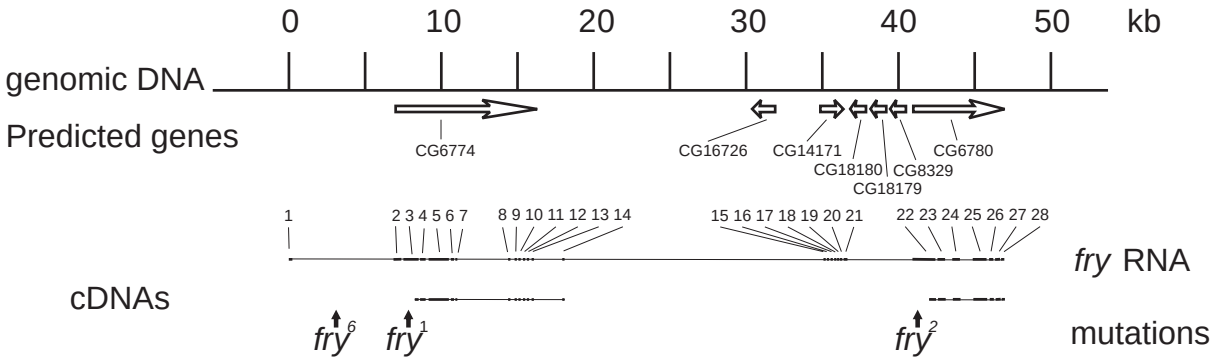

Fig. 1. A map of the *fry* gene. A 50 kb segment is shown. The BDGP/Celera collaboration has predicted seven genes in this region. Three of these (CG6774, CG14171 and CG6780) largely comprise the *fry* gene. The other four are transcribed on the complementary strand and have not been studied. The relative location and size of the 28 *fry* exons are shown. cDNA clones have been found in two regions. One group of cDNA clones was near the 5′ end of the transcript. The longest of these was about 4 kb and it included sequences from exons 3-14. A second cDNA was found as an EST (SD10447) and is located at the 3′ end of the gene. Southern blot analysis and DNA sequencing were used to determine the locations of three *fry* mutations. The P insertion responsible for fry^6 was inserted into the first intron of *fry*. The fry^1 mutation is a frameshift mutation in exon 3. The fry^2 mutation is a nonsense mutation in exon 22.

field microscopy using approaches described previously (Wong and Adler, 1993).

Statistical analysis

The Sigma Stat program (Jandel) was used for comparing different genotypes or treatments.

RESULTS

Identification and recovery of *fry* mutations

In a screen to recover new wing hair polarity mutants, we recovered five EMS-induced alleles of an essential gene we named *furry* (*fry*). Clones of *fry* mutant cells produce a dramatic multiple hair cell phenotype. A more detailed description of this and other *fry* phenotypes is provided below. The *fry* mutations were uncovered by *Df(3L)AC1* (67A5; 67D7-13) but not *Df(3L)29A6* (66F5; 67B1) localizing it to 67B-D. We screened P insertion alleles in this region and identified one *l(3)02240* that failed to complement *fry* point mutations. We confirmed that the P insertion was responsible for the *fry* mutation, as it was induced to revert at a high frequency by P transposase. In addition to complete revertants, many partial revertants were recovered that displayed a weak *fry* phenotype. This P insertion mutation has been described as being in a suppressor of the rough eye phenotype that results from driving the expression of *sina* using the GMR promoter (Neufeld et al., 1998). We confirmed that *Df(3L)AC1* suppressed this gain-of-function phenotype, but we did not see any suppression from the P insertion allele or with any of our EMS induced *fry* alleles.

All of the EMS-induced alleles and the P insertion allele (fry^6) were recessive lethals. The EMS alleles (as homozygotes, hemizygotes or heteroallelic heterozygotes) typically died as second or third instar larvae with only occasional animals surviving until the prepupal period. Animals that were homozygous for the fry^6 P insertion allele often died as pharate adults that displayed a strong *fry* phenotype. Heteroallelic combinations that contained fry^6 displayed a similar phenotype.

We used fry^7, a weak viable partial revertant of fry^6, in an attempts to distinguish between the severity of the EMS-induced alleles. In heteroallelic heterozygotes with fry^7, three of the four extant EMS alleles resulted in a phenotype that was indistinguishable from the phenotype seen in fry^7/Df wings. Thus, at least for this phenotype these alleles are phenotypic null alleles. One of the EMS-induced alleles (fry^4) and the P insertion allele (fry^6) appeared to be hypomorphic alleles.

The molecular characterization of *fry*

We used the P insertion mutation as a tag to identify *fry* DNA. We analyzed the DNA region surrounding the P insertion allele by DNA sequencing, sequence analysis, RT-PCR, cDNA clone analysis and the sequencing of mutant alleles (details are presented in the Materials and Methods). The P element in fry^6 was inserted into the first intron of *fry* (Fig. 1). Genomic Southern blot analyses showed this P was lost in all four of the fry^6 revertants examined (data not shown). Several partial revertants were examined and in each the P element remained but was altered in structure.

Evidence was obtained for two distinct *fry* mRNAs from cDNA clone and RT-PCR. One of these (*fry-l*) was encoded by 28 exons spread out over 46 kb of genomic DNA (Fig. 1). The exons were clustered in three regions along the chromosome. Conceptual translation of this mRNA resulted in a 3479 amino acid open reading frame (AAG41424). We also found evidence for a second form of this mRNA (*fry-s*) that differed by use of an alternative 5′ splice site for the 14th intron of *fry*. Conceptual translation of this alternative splice form resulted in an ORF of 1629 amino acids, as there is a stop codon early in the extended exon 14. The first 1623 of these would be identical to those in Fry-L. Based on RT-PCR analysis, this splice form shares downstream exons with *fry-l* (but not exon 15), but these exons are downstream of a stop codon in the extended exon 14 and thus would not encode protein. Given the size and complexity of the *fry* transcription unit, it remains possible that there are additional splice forms of the *fry* mRNA that we did not uncover. We sequenced the open reading frame from two EMS-induced *fry* alleles. In fry^1, we found a 1 bp deletion in exon 3, resulting in a frameshift mutation that scrambles the amino acid sequence after amino acid 403. In fry^2 we found a nonsense mutation in exon 22 that truncates

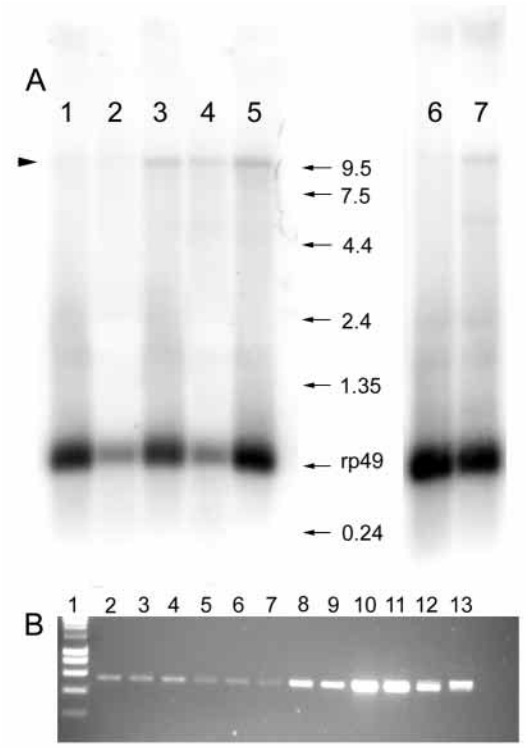

Fig. 2. (A) A northern blot hybridized with 5′ and 3′ probes for both forms of the *fry* cDNA. The location of RNA size markers is indicated. Lane 1 contained approximately 2.5 μg of fry^6/fry^6 1-2 day pupal poly(A)$^+$ RNA. Lane 2 contained 40 μg of fry^6/fry^6 1-2 day pupal total RNA. Lane 3 contained approximately 2.5 μg of 1-2 day Oregon R pupal poly(A)$^+$ RNA. Lane 4 contained 40 μg of 1-2 day Oregon R total RNA. Lane 5 contained 2.5 μg of adult head poly(A)$^+$ RNA. The filter containing lanes 1-5 was probed simultaneously with a probe for the 5′ region of the *fry* mRNA and a probe for the approximately 500 bp *rp49* mRNA as a loading control. Lane 6 contained approximately 2.5 μg of fry^6/fry^6 1-2 day pupal poly(A)$^+$ RNA and lane 7 contained approximately 2.5 μg of 1-2 day Oregon R pupal poly(A)$^+$ RNA. This filter was probed simultaneously with a probe for the 3′ region of *fry* and with a probe for *rp49* as a loading control. (B) PCR amplification of a region of the *fry* mRNA from a panel of *Drosophila* cDNAs made from a variety of developmental stages (Origene Technologies). Lane 1 is a size marker, lane 2 contains cDNA from 0-4 hour embryos, lane 3 from 4-8 hour embryos, lane 4 from 8-12 hour embryos, lane 5 from 12-24 hour embryos, lane 6 from 1st instar larvae, lane 7 from 2nd instar larvae, lane 8 from 3rd instar larvae, lane 9 from pupae, lane 10 from male heads, lane 11 from female heads, lane 12 from male bodies and lane 13 from female bodies. The fragment amplified is found in both *fry-l* and *fry-s*.

the Fry-L protein after amino acid 2298. As the fry^2 mutation is a strong allele and does not affect the Fry-S protein, we conclude that Fry-L has an important function in the development of hairs, bristles and laterals. The data do not prove that Fry-S also has a function in these cell types. The sequence data confirmed that we had identified the *fry* gene.

The existence of a large *fry* mRNA (>10 kb) was confirmed by northern blot analysis (Fig. 2A). This band was reduced in amount (and perhaps slightly larger in size) in the fry^6 homozygous pupae (P allele). Only one band was seen on a northern blot with either a 5′- or 3′-specific probe, consistent with both splice forms being of similar size (or one being much rarer than the other). We used RT-PCR to examine the developmental distribution of the *fry* mRNA (Fig. 2B). *fry* mRNA was seen in cDNA preparations from all developmental stages examined. It was most abundant in adult heads.

The BDGP/Celera analysis of the *Drosophila* genome sequence predicted three independent genes that we have found to comprise the *fry* transcription unit (Adams et al., 2000). These are the genes CG6774, CG14171 and CG 6780 (Fig. 1). The genome project predicted 4 genes that are located in introns of *fry*. All of these predicted genes are transcribed on the opposite strand of DNA from *fry*.

The Fry protein is a conserved protein

Fry is a member of a conserved family of proteins found in mammals, *C. elegans*, *Arabidopsis* and yeast (Fig. 3). The similarity is concentrated in five regions separated by short regions of little or no similarity. The similarity is highest in the N-terminal most region that we call the *fry* domain. In this 630 amino acid region, the Fry and the human CAB4244 protein are 63% identical and 79% similar. The fly, human and worm proteins contain all five of the similarity regions, suggesting these regions may represent functional domains. The *Arabidopsis* and yeast proteins only contain the first three similarity regions. Several additional database sequences share similarity to part of the C-terminal region of Fry. These sequences are likely to represent partial cDNAs. The Fry-S protein contains the Fry domain and about half of the second homology segment. It is unclear whether other organisms produce a protein that is equivalent to the Fry-S protein.

The Fry proteins do not contain any protein motifs that are insightful with regard to function. There is no information about the biological function of the homologs, as all were found in genome or EST sequencing projects. The homolog from yeast (Tao3) has been found to be nonessential. Two phenotypes have been identified with the knockout of this gene. One is altered transcription of the OCH1gene and the second is the clumping of mutant cells (*Saccharomyces* Genome Database).

Wing hair phenotype

We examined the phenotype of strong *fry* alleles in mitotic clones in adult wings (Fig. 4, see also Fig. 9). Even small clones induced in all regions of the wing showed a strong phenotype, indicating that *fry* needs to function in all wing cells. Most *fry* cells formed a cluster of hairs and we could see examples of hairs that were split distally. On average, the *fry* clone cells produced 5.7 hairs per cell (a branched hair with two distal ends was counted as two hairs in these experiments), although the cellular phenotype was quite variable and some cells formed more than a dozen hairs. The *fry* hairs were often almost orthogonal to the wing surface, appearing as dots in the light microscope. A similar phenotype was seen in pharate adults that were homozygous or hemizygous for the fry^6 allele (Fig. 4C,D). Weaker versions of this phenotype were seen on the wings of fry^7/fry^x (where *x* is any of the EMS alleles) flies. Based on the phenotype seen in clones, it appeared quite likely that *fry* acted cell autonomously, but to test this in a rigorous way we induced clones marked by the loss of the N-Myc epitope tag and examined these in pupal wings that were also stained to show the actin cytoskeleton. In all cases, only clone

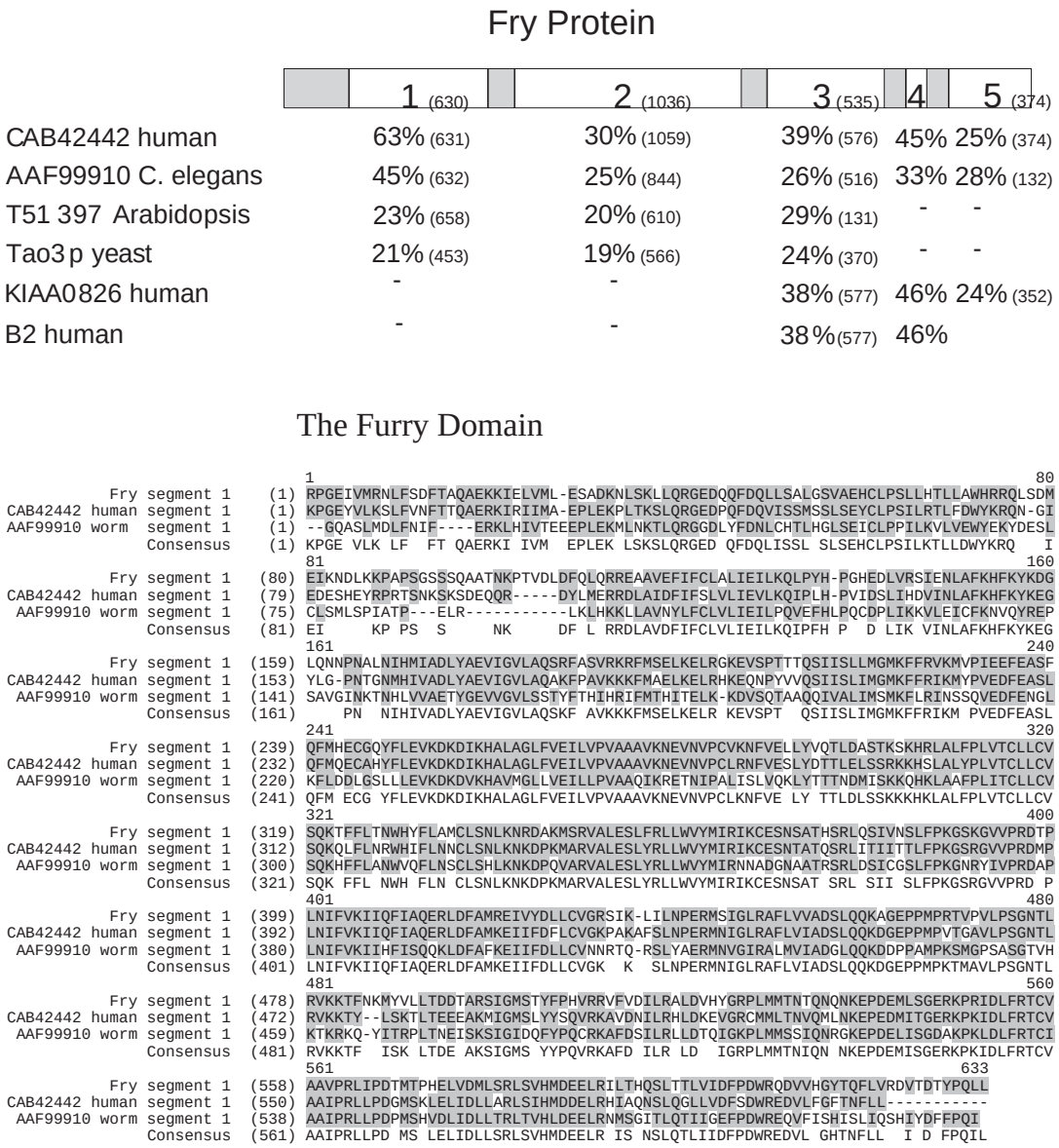

Fig. 3. (Top) Diagrammatic representation of the Fry-L protein with the five similarity regions labeled. In parentheses is the number of amino acids in that region of the Fry protein. Shown below the Fry protein is the percentage of identical amino acids in various Fry homologs. For each of these, the number of amino acids over which the similarity to Fry is seen is given in parentheses. Note for all of the proteins that contain the 4th region, it is approximately 110 amino acids. (Bottom) Amino acid sequence for Fry, CAB42442 and AAF99910 for the first similarity domain. We call this region the Fry domain. Similar amino acids are shaded and a consensus sequence is also shown.

cells showed a mutant phenotype confirming that *fry* acted cell autonomously in all regions of the wing (Fig. 4B). We also examined the wings of fry^6 homozygous flies and found that late in hair development (>36 hours after white pupae) the phenotype resembled that seen in adult wings (Fig. 4D). At earlier times (e.g. 33 hours after white pupae) the phenotype seemed somewhat weaker, suggesting that the hair splitting occurred progressively throughout hair morphogenesis. This is similar to what we had seen previously in *trc* (Geng et al., 2000). Compelling evidence for the phenotype getting more severe as development proceeded was obtained for arista laterals, as described in some depth below. It is worth noting that *fry* hairs stained as strongly for F-actin, as did wild-type hairs.

Bristle phenotype

We primarily examined the *fry* bristle phenotype in pharate adults of strong hypomorphic genotypes that contained fry^6. A wide range of bristle phenotypes was seen (Fig. 5). In all body regions, some bristles were indistinguishable from wild type (Fig. 5A). In the abdomen, legs, notum and triple row on the wing, the most common phenotype was the presence of one or a few locations where the bristle was branched (Fig. 5A,C). Such bristles were relatively normal in shape and length except for the branching. In some cases, several branches were seen at the same proximal/distal location along the shaft. Bristles with extensive splitting were occasionally seen and these were often shorter than normal. There were also some bristles that were bent, distorted and shorter than normal without being extensively split (Fig. 5B). This was common only on the head. We examined developing bristles in *fry* pupae, where we stained the actin cytoskeleton. The phenotypes seen overlapped those seen in *fry* adult bristles. The large bundles of actin filaments seen in wild-type bristles were present in *fry* bristles, but some abnormalities were seen. In some bristles, the bundles appeared to become disorganized distally, so that there was no longer a series of parallel bundles (Fig. 5E). This is similar to the phenotype that is induced by treating cultured thoraces with

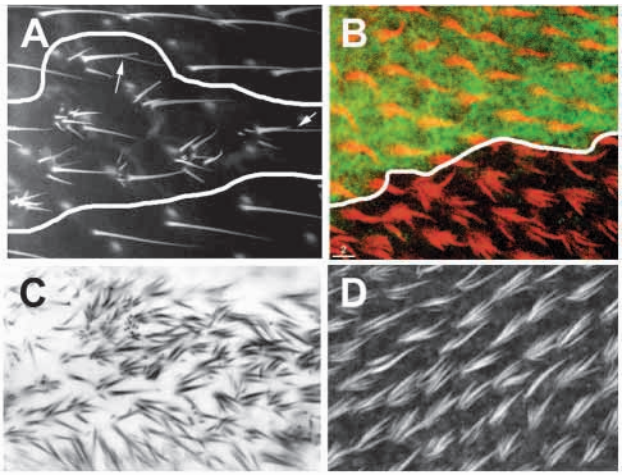

Fig. 4. The wing phenotype of *fry*. A shows a fry^1 clone seen in the SEM. This micrograph was taken of an adult wing mounted on a stud without any metal coating. The clone boundary is outlined in white. The arrows point to hairs split distally. This is shown at approximately twice the magnification of the adult cuticle in C. (B) A fry^2 clone in a pupal wing stained with an anti-actin antibody to stain the developing hairs. The clone is marked by the loss of expression of the N-Myc epitope (clone cells do not stain green). The clone boundary is outlined in white. Note that only the clone cells show a *fry* mutant phenotype. A 2 μm size marker is shown. (C) A wing from a fry^6/fry^6 pharate adult. Note the strong *fry* mutant phenotype. (D) A confocal image of a fry^6/fry^6 pupal wing stained with Alexa 488 phalloidin to stain the actin cytoskeleton (this micrograph is shown at the same magnification as B).

the broad-spectrum kinase inhibitor stauroporine (Tilney et al., 2000a). In some cases we found pupal bristles where the shaft was clearly split (Fig. 5D). In these bristles, most bundles of actin filaments were continuous both proximally and distally from the branch-point.

Arista phenotype

In weak *fry* genotypes that were adult viable, we found frequent branched arista laterals. Except for the branching, the morphology of the laterals was close to normal. In some cases, mutant laterals appeared slightly thinner than normal in distal regions and/or slightly curled. The overall phenotype was similar to that of weak *trc* mutants (Geng et al., 2000). In pharate adults homozygous or hemizygous for fry^6 a stronger lateral phenotype was seen (Fig. 6B). There was extensive branching of essentially all laterals and the weak distal curling and thinning phenotype noted above was more noticeable. Many of the branches were very thin and only visible at higher magnification (see Fig. 6B insert). Equivalent observations were made on developing laterals in pupae (Fig. 6D). As was noted for hairs and bristles above the actin staining of developing laterals was strong and equivalent to that seen in wild type.

The antenna is located at the anterior end of the pupae and we have found it possible to image developing laterals in vivo by cutting a window in the pupal case. We used this approach to determine the timing and properties of splitting laterals in weak *fry* mutants (fry^7) (Fig. 7). In describing these data we have paid particular attention to the locations of the branch-points and the lateral segments distal to the branch-points (we

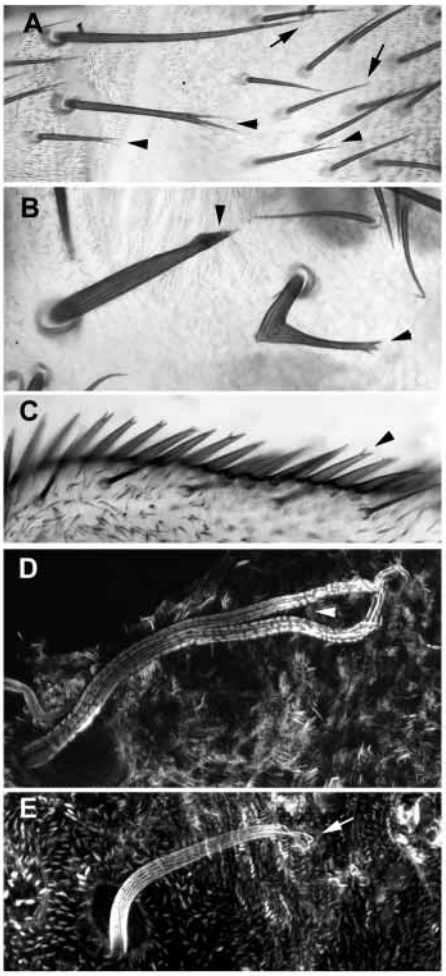

Fig. 5. The bristle phenotype of *fry*. All panels show fry^6 homozygous animals. (A) Abdominal bristles from a pharate adult. Both split (arrowheads) and normal (arrows) looking bristles can be seen. Note that except for the location of the branchpoint the mutant bristles have a normal shape. (B) Several large bristles on the head of a pharate adult. These illustrate the abnormal shape seen in bristles in this region. (C) Part of the triple row from the anterior margin of the wing. Many of the stout bristles are split distally (arrowhead). (D) A confocal image of a phalloidin stained head bristle. This bristle has already started to break down actin filaments, which now appear as short segments. The bristle shows a branch (arrowhead) midway along its length. Note that actin filaments can be seen running from proximal to distal across the branch. (E) A bristle where the actin filaments become disorganized near the distal tip (arrow).

refer to these as arms) and their distance from the central core of the arista. Substantial variation was seen in the natural history of lateral splitting. In this set of experiments, branched laterals could be put into one of two phenotypic groups. It is notable that branched laterals typically did not grow dramatically more slowly than normal laterals in the same pupae (either ipsilateral or contralateral).

The most common observations were examples (15/18 laterals (from 17 aristae and 14 pupae)) where an elongating lateral was normal when first seen but where it subsequently split at or near the distal tip (Fig. 7, right). In these cases, it is possible that the branching was a result of an abnormality at the lateral tip. This could happen at any time during lateral

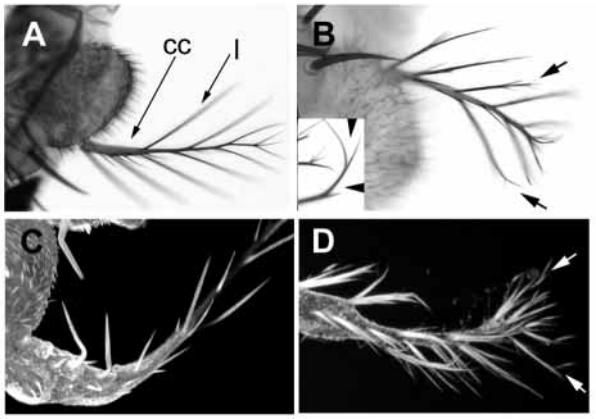

Fig. 6. (A,B) Brightfield images of adult aristae; (C,D) Confocal projections of Alexa 488-phalloidin stained pupal aristae. (A,C) Wild-type aristae; (B,D) *fry*^{6} homozygous aristae. Large arrows point to locations of split laterals. The insert in B is a higher magnification image of a *fry*^{6} homozygous arista. Note the fine branches on the lateral. cc, the central core of the arista; l, a lateral.

elongation. As morphogenesis proceeded, both of the resulting arms continued to elongate, and the location of the branch-point also moved distally. The relative extent of branch-point movement (i.e. distance from the central core to the branch-point) compared with arm elongation was quite variable. Typically, the extent of branch-point movement was much greater than that of arm elongation, as was the case for the lateral shown in Fig. 7 (right side). The relative extent of arm elongation was also variable. In some cases both arms elongated similar extents, while in other cases one grew more than the other.

A second pattern for lateral branching was the de novo formation of a new arm well proximal to the distal tip (Fig. 7, left side; 3/18 cases – all three from separate animals). In these cases, it is likely that the branching is due to a fraying of the lateral. We sometimes saw a bend or bulge in the lateral at the location of a future branch. As was seen when the branching took place near or at the elongating tip, both of the resulting arms typically continued to elongate and the location of the branch-point moved distally. Once again there was substantial variation in the relative extent of elongation.

fry is not part of the *fz* pathway but probably functions in the same process as *trc*

Mutations in a number of genes such as *multiple wing hairs* (*mwh*), *fuzzy* (*fy*) and *ultrahairA* (*ultA*), which are thought to function in different processes result in a multiple hair cell phenotype (Wong and Adler, 1993; Turner and Adler, 1998; Eaton et al., 1996; Geng et al., 2000; Adler et al., 2000). We addressed the possibility that *fry* functioned in the same pathway as several of these genes using a genetic test. If mutations were in genes that encoded components of a linear pathway, then a double null mutant should not have a more severe phenotype than the most severe single mutant. However, if two genes function in parallel pathways, then a double null mutant might display an additive or synergistic phenotype.

One group of genes where mutations have multiple hair cell phenotypes are downstream components of the *fz* pathway in the wing such as *multiple wing hairs* (*mwh*; Wong and Adler, 1993; Shulman et al., 1998). We used FLP/FRT to generate *mwh fry*^{1} wing clones and found that these had a much stronger phenotype than either single mutant (*mwh* clones had 3.54 hairs/cell (Fig. 8E); *fry*^{1} had 5.7 hairs/cell (Fig. 8A)) consistent with these genes being in parallel pathways. The large number of very small hairs formed by cells in these clones were difficult to count, but we estimate that on average the clone cells contained more than 15 hairs/cell (Fig. 8F; our actual

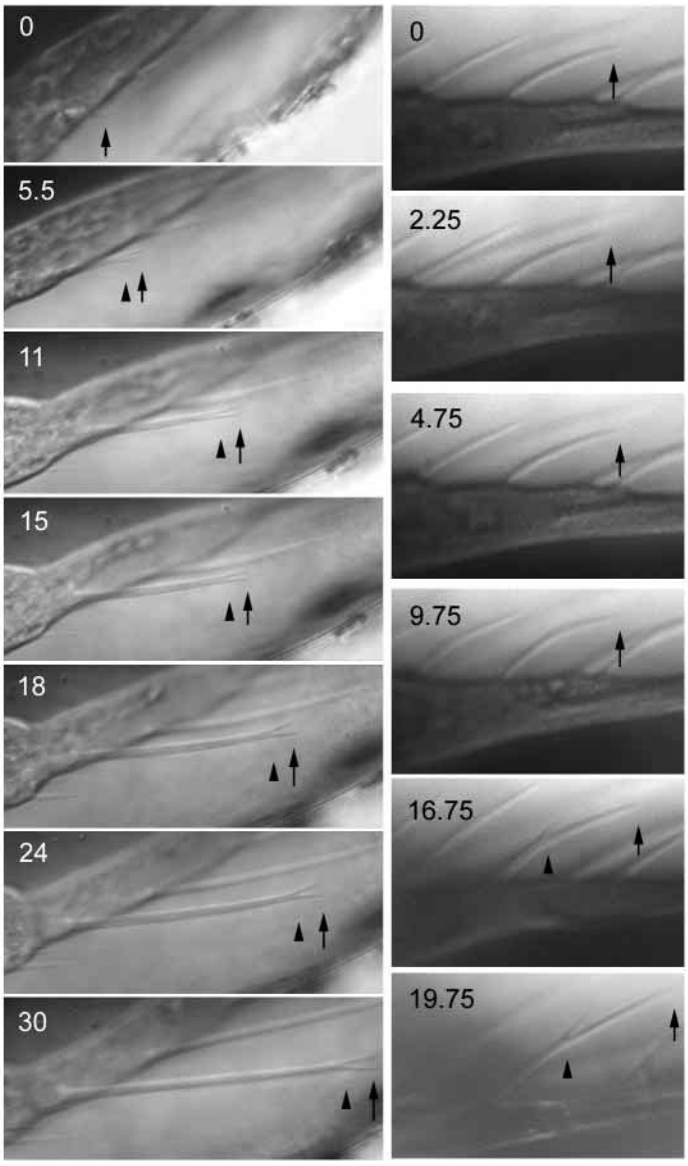

Fig. 7. A set of images taken of developing *fry*^{7} laterals over time. As the developmental rate of *fry*^{7} animals is delayed and variable, we note the first panel as 0 hours and report the number of hours since that time. Two time series are shown – one on the right and the other on the left. The arrows point to the most distal point on the lateral of interest, the arrowhead to the relevant branch-point. In the panels on the right, note the dramatic movement of the branch-point as the lateral grew. In the panels on the left, note the deformation of the lateral at 9.75 hours and its subsequent split by 16.75 hours.

count was 16.35 hairs/cell). We also generated *fry*^{1} mutant clones in *fuzzy* and *fritz* mutant wings (Collier et al., 1997; Collier and Gubb, 1997). Once again we found the doubly mutant (e.g. *fy*; *fry*) cells had a stronger phenotype than either single mutant (data not shown).

Mutations in the *trc* gene result in a multiple hair cell phenotype that is quite similar to that of *fry* (compare Fig. 8A with C; Geng et al., 2000). Clones of *fry*^{1} *trc*^{7} mutant cells did not show a stronger phenotype (Fig. 8D) than the single mutants (*fry*^{1} *trc*^{7} clones had 5.37 hairs/cell and *trc*^{7} 5.74 hairs/cell (P=0.46, t-test)). This is in sharp contrast to what we saw for *mwh fry*^{1} mutant cells. This suggests that *fry* and *trc* may function in the same pathway. As a further test of this hypothesis, we also examined *mwh trc*^{7} clones. As expected, we found the *mwh trc*^{7} cells had a much stronger phenotype than either single mutant alone (Fig. 8B).

DISCUSSION

fry does not function in the *fz* pathway, but probably functions in the same pathway as *trc*

The detailed morphology of *fry* mutant cells is indistinguishable from *trc* mutant cells, suggesting they might function in the same cellular process. Consistent with this hypothesis, we found that cells doubly mutant for *fry* and *trc* showed a phenotype that was indistinguishable from either single mutant. Previous data has shown that *trc* encodes the *Drosophila* NDR kinase (Geng et al., 2000). This raises the possibility that *fry* might encode a substrate for this kinase or a protein involved in modulating *trc* activity. A target peptide sequence for the human NDR kinase has been reported (Millward et al., 1995), but this sequence is not found in Fry. However, as Millward and colleagues noted, this synthetic peptide does not appear to be an optimal substrate for NDR.

Mutations in genes such as *mwh*, a downstream component of the *fz* pathway in the wing, also gives rise to multiple hair cells (Wong and Adler, 1993). The morphology of these differs from the *fry* mutant cells in a number of ways. Notably, in *fry* the multiple hairs are clustered more tightly, there is much more evidence of splitting. Furthermore, the prominent polarity abnormalities of genes such as *mwh* are missing in *fry*. We found that *mwh fry*^{1} cells had a much stronger phenotype than either single mutant, a result that stands in sharp contrast to the lack of additivity for the *fry* and *trc*. We interpret this result as *mwh* causing the formation of multiple independent prehair initiation sites and each of these giving rise to a cluster of hairs due to the *fry*-dependent splitting. Indeed the phenotype of the doubly mutant cells approximated the multiplicative phenotype this model predicts. Similar results were also found for *mwh trc*^{6} mutant cells. We also carried out similar experiment where we induced *fry* clones in a *fy* (Collier et al., 1997) or *frtz* (Collier and Gubb, 1997) mutant background. These two genes, which also appear to be components of the *fz* pathway in the wing have a much weaker multiple hair cell phenotype than *mwh*. In both of these cases we found the doubly mutant cells also had a stronger phenotype than either single mutant.

fry mutations result in the splitting of arista laterals

The *fry* phenotype in wing hairs, bristles and arista laterals shows striking similarities, suggesting a common mechanism is involved. Observations on developing pupal aristae showed that in *fry* mutants, laterals can split at a variety of stages. The splitting can be early or late in lateral morphogenesis, near the distal tip or far from it. Observations on fixed pupal bristles and adult cuticular bristles suggest this is the case in this cell type as well. This argues that *fry* functions to maintain the integrity of these structures during their morphogenesis. The function of *fry* does not appear to be absolutely essential for their morphogenesis, as at least some bristles in *fry* mutants are indistinguishable from wild type. The situation is less clear for wing hairs, as many *fry* cells produce clusters of hairs with only a minority of hairs being obviously split. It is possible that a lack of *fry* function could cause the formation of independent hair initiation centers in wing cells or to hair initiation centers that are too large to ensure a single hair is formed (Adler et al., 2000). It would not be surprising if the assembly and crosslinking properties of actin and tubulin might function to reduce the size of an initiation center to insure that a single hair was formed. *fry* mutations could interfere with this process, leading to a larger center and hair clusters. Alternatively the clusters could be due to splitting that occurs early in hair morphogenesis or the splitting of the initiation center prior to actual hair outgrowth. This latter hypothesis provides a

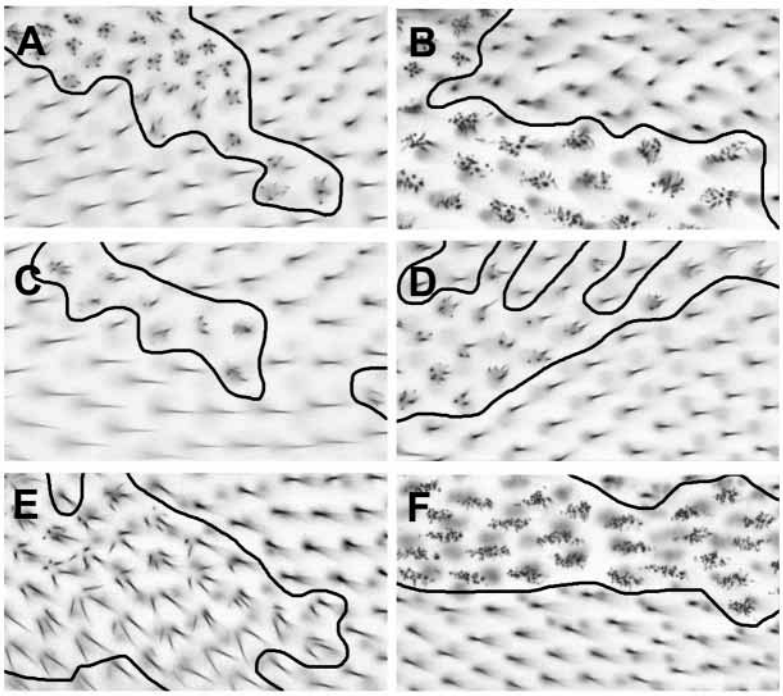

Fig. 8. Analysis of *fry* in wing clones. (A) A light micrograph of a region of a wing with a *fry*^{1} *w*ing clone (outlined in black). (B) A *mwh trc*^{7} clone. (C) A *trc*^{7} clone. (D) A *fry*^{1} *trc*^{7} clone. (E) A *mwh* clone. (F) A *mwh fry*^{1} clone. Note the extreme phenotypes in the *mwh trc*^{7} and *mwh fry*^{1} clones. They are much stronger than either single mutant. Also note that the *fry*^{1} *trc*^{7} clone does not show a stronger phenotype than either single mutant.

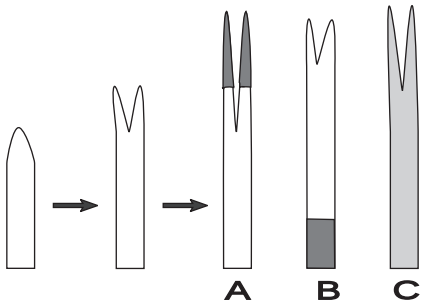

Fig. 9. Three models for the growth and splitting of laterals are shown (A-C). A lateral is shown before and after splitting near the distal tip. The expectation if subsequent growth is restricted to the distal tip, the proximal end or occurs throughout the length of the lateral, respectively. The shaded area represents material added by growth after splitting. Note that in A, the length of the arms distal to the split increases but there is no change in the distance from the branch-point to the proximal end. In B, the arms do not change length, but the distance from the branch-point to the proximal end increases. In C, growth takes place throughout the lateral. In this case we predict an increase in the length of the arms distal to the branch-point and an increase in the distance from the branch-point to the proximal end. Our observations on *fry* arista laterals are consistent with C.

common explanation for the phenotypes seen in all three cell types, hence is in some ways more appealing.

The morphology of branched hairs, laterals or bristles is typically normal except for the region of the branch point. This suggests that *fry* does not encode an integral component of these cellular extensions. In this way, *fry* and *trc* differ in a fundamental way from mutations in actin cytoskeleton components such as *crinkled* (Ashburner et al., 1999; Kiehart et al., 1999), *sn* (Cant et al., 1994) or *f* (Petersen et al., 1994), which result in abnormal morphology in all regions of the structure. We previously suggested that *trc* might encode a component of a system that either coordinates or organizes the growth of different subcellular components during morphogenesis (e.g. membrane, actin cytoskeleton, etc.), or monitors the 'quality' of the developing structure to insure its integrity (i.e. it functions in a pathway that is analogous to a morphogenetic checkpoint; Geng et al., 2000). It would also be appealing to explain the function of *fry* in the same way.

The cell biology of lateral growth

The outgrowth of a cellular extension is a feature of many cells. In several systems, studies on the mechanisms of elongation has led to the conclusion that the polymerization of actin at the membrane drives extension (Alberts et al., 1994). Indeed, the ultrastructure of actin bundles in developing bristles argues that the large bundles of actin filaments are assembled in smaller units at the distal tip of the elongating bristle (Tilney et al., 1996). It is not clear, however, how other cellular components (e.g. plasma membrane) are added to such outgrowths. A model of growth only from the tip does not easily accommodate our observations on split elongating laterals (Fig. 9). If growth were only from the tip, then we would not expect the branch-point to move distally as growth proceeded; however this was a routine and prominent result. We note however, that a similar distal movement of 'blebs' was reported in a classic paper on the growth of the Thyone acrosomal process (Tilney and Inoue, 1982). This is an example where actin polymerization at the tip is believed to drive extension. In addition, our observations do not support a simple model of growth being restricted to the proximal base of the lateral. In this case we would not expect the length of an arm distal to a branch-point to grow but this was also routinely seen. These data could be explained by growth taking place at both the distal and proximal ends of the lateral; however, this model cannot explain an increase in the distance between branch-points on multiply branched laterals. Such multiply branched laterals were rare in the fry^7/fry^1 mutants examined, but they were seen frequently in equivalent experiments on *trc* mutants where multiple branch-points are much more common (P. N. A., unpublished). The data can most simply be explained by growth taking place at all locations along the proximal distal axis of the laterals. An alternative hypothesis is that growth is normally from the tip and that growth throughout the lateral is a consequence of the *fry* mutation. The examination of additional 'split lateral' mutants should determine if this latter hypothesis is tenable. It remains to be established whether all cellular components are added to a growing lateral (or bristle) in the same way. It should be possible to follow the addition of different cellular components by the induction of transgenes that encode tagged proteins during lateral elongation (e.g. GFP-actin). For example, if actin is added only at the tip we predict that the tip will be the principal location of GFP fluorescence shortly after transgene induction. Such experiments are in progress.

This work was supported by a grant from the NIH (GM53498) to P. N. A.

REFERENCES

Adams, M. D., Celniker, S. E., Holt, R. A., Evans, C. A., Gocayne, J. D., Amanatides, P. G., Scherer, S. E., Li, P. W., Hoskins, R. A., Galle, R. F. et al. (2000). The genome sequence of Drosophila melanogaster. *Science* **287**, 2185-2195.

Adler, P. N., Liu, J. and Charlton, J. (2000). Cell size and the morphogenesis of wing hairs in Drosophila. *Genesis* **28**, 82-91.

Alberts, B., Bray, D., Lewis, J., Raff, M., Roberts, K. and Watson, J. D. (1994). *Molecular Biology of the Cell*. New York: Garland Publishing.

Ashburner, M., Misra, S., Roote, J., Lewis, S. E., Blaszej, R., Davis, T., Doyle, C., Galle, R., George, R., Harris, N. et al. (1999). An exploration of the sequence of a 2.9 Mb region of the genome of Drosophila mealnogaster. The Adh region. *Genetics* **153**, 179-219.

Brown, N. H. and Kafatos, F. C. (1988). Functional cDNA libraries from Drosophila embryos. *J. Mol. Biol.* **203**, 425–437.

Bryan, J., Edwards, R., Matsudaira, P., Otto, J. and Wulfkuhle, J. (1993). Fascin, an echinoid actin-bundling protein, is a homolog of the Drosophila singed gene product. *Proc. Natl. Acad. Sci. USA* **90**, 9115-9119.

Cant, K., Knowles, B. A., Mooseker, M. S. and Cooley, L. (1994). Drosophila *singed*, a fascin homolog, is required for actin bundle formation during oogenesis and bristles extension. *J. Cell Biol.* **125**, 369-380.

Collier, S. and Gubb, D. (1997). Drosophila tissue polarity requires the cell-autonomous activity of the fuzzy gene, which encodes a novel transmembrane protein. *Development* **124**, 4029-4037.

Collier, S., Tree, D., Johnson, G. and Adler, P. (1997). Characterization of the fuzzy gene product and a new tissue polarity gene fritz. *Dros. Res. Conf.* **38**, 147A.

Eaton, S., Wepf, R. and Simons, K. (1996). Roles for Rac1 and Cdc42 in planar polarization and hair outgrowth in the wing of Drosophila. *J. Cell Biol.* **135**, 1277-1289.

Geng, W., He, B., Wang, M. and Adler, P. N. (2000). The tricornered gene, which is required for the integrity of epidermal cell extensions, encodes the Drosophila Nuclear DBF2-related kinase. *Genetics* **156**, 1817-1828.

Golic, K. G. and Lindquist, S. (1989). The FLP recombinase of yeast catalyzes site-specific recombination in the Drosophila genome. *Cell* **59**, 499-509.

He, B. and Adler, P. N. (2001). Cellular mechanisms in the development of the Drosophila arista. *Mech. Dev*. **104**, 69-78.

Kiehart, D. P., Montague, R. A., Roote, J. and Ashburner, M. (1999). Evidence that crinkled, mutations in which cause numerous defects in Drosophila morphogenesis, encodes a myosin VII. *Dros. Res. Conf.* **40**, 295C.

Millward, T., Cron, P. and Hemmings, B. A. (1995). Molecular cloning and characterization of a conserved nuclear serine(threonine) protein kinase. *Proc. Natl. Acad. Sci. USA* **92**, 5022-5036.

Neufeld, T. P., Tang, A. H. and Rubin, G. M. (1998). A genetic screen to identify components of the sina signaling pathway in Drosophila eye development. *Genetics* **148**, 277-286.

Petersen, N. S., Lankenau, D. H., Mitchell, H. K., Young, P. and Corces, V. G. (1994). forked proteins are components of fiber bundles present in developing bristles of Drosophila melanogaster. *Genetics* **136**, 173-182.

Shulman, J. M., Perrimon, N. and Axelrod, J. D. (1998). Frizzled signaling and the developmental control of cell polarity. *Trends Genet.* **14**, 452-458.

Tilney, L. G. and Inoue, S. (1982). Acrosomal reaction of thyone sperm II. The kinetics and possible mechanism of acrososmal process elongation. *J. Cell Biol.* **93**, 820-827.

Tilney, L. G., Tilney, M. S. and Guild, G. M. (1995). F actin bundles in Drosophila bristles. I. Two filament cross-links are involved in bundling. *J. Cell Biol.* **130**, 629-638.

Tilney, L. G., Connelly, P., Smith, S. and Guild, G. M. (1996). F-actin bundles in Drosophila bristles are assembled from modules composed of short filaments. *J. Cell Biol.* **135**, 1291-1308.

Tilney, L. G., Connelly, P. S., Vranich, K. A., Shaw, M. K. and Guild, G. M. (1998). Why are two cross-linkers necessary for actin bundle formation in vivo and what does each cross-link contribute? *J. Cell Biol.* **143**, 121-133.

Tilney, L. G., Connelly, P. S., Vranich, K. A., Shaw, M. K. and Guild, G. M. (2000a). Actin filaments and microtubules play different roles during bristle elongation in Drosophila. *J. Cell Sci.* **113**, 1255-1265.

Tilney, L. G., Connelly, P. S., Vranich, K. A., Shaw, M. K. and Guild, G. M. (2000b). Regulation of actin filament cross-linking and bundle shape in Drosophila bristles. *J. Cell Biol.* **148**, 87-100.

Turner, C. M. and Adler, P. N. (1998). Distinct roles for the actin and microtubule cytoskeletons in the morphogenesis of epidermal hairs during wing development in Drosophila. *Mech. Dev.* **70**, 181-192.

Wong, L. L. and Adler, P. N. (1993). Tissue polarity genes of Drosophila regulate the subcellular location for prehair initiation in pupal wing cells. *J. Cell Biol.* **123**, 209-221.

Xu, T. and Rubin, G. M. (1993). Analysis of genetic mosaics in developing and adult Drosophila tissues. *Development* **117**, 1223-1237.